

# Autonomous Swing-Angle Estimation for Stable Slung-Load Flight of Multi-Rotor UAVs\*

Seung Jae Lee and H. Jin Kim

**Abstract**—This paper presents a practical swing-angle estimation method for slung load operations of the multi-rotor unmanned aerial vehicle (UAV), which is essential to maintain the safety during the operation. In order not to rely on extra sensors for monitoring the swing angle, the proposed method in this paper offers an autonomous swing-angle estimation using only an inertial measurement unit (IMU) and a single load cell attached to the slung load. The disturbance observer (DOB) derived external force estimation is performed to estimate the swing angle. The unique structure of the proposed DOB-based disturbance force estimation technique utilizes the IMU data only. Both simulation and actual experiment are performed to validate the feasibility of the proposed algorithm.

## I. INTRODUCTION

Slung-load transportation is a valuable application of vertical take-off and landing platforms, such as a helicopter that needs to carry oversized freight[1]. It is also applicable to delivery using multi-rotor unmanned aerial vehicles (UAVs) since their fuselage is mostly too small to carry a bulky package.

When the UAV is hanging a freight as a slung load, the oscillation is inevitable where the freight pulls the UAV towards the direction of the tether, causing undesirable motion. This undesirable motion is a more critical issue to the autonomous UAV flight compared to the manual flight. When the operator controls the attitude and thrust of the UAV (e.g. a piloted helicopter or manual control) during the oscillation of the slung load, the stability augmentation system (SAS) is applied only to the attitude control. Therefore, there is no force generation for UAV to recover its desired position. However, the autonomous position controlled UAV tries to move towards the opposite direction of the pulling force generated by the slung load for position recovery, taking a chance to increase the oscillation of the slung load. It is a very dangerous situation for the UAV since the increasing oscillation causes a larger horizontal disturbance force and makes the UAV generate a larger force to recover the desired position, which may lead to instability of the overall system.

The stability issue of the autonomous slung-loaded UAV has been addressed by many researchers[2][3][4]. The mainstream of the research is to move the UAV's position properly to damp the swing angle of the oscillation. These in common require the measurement of the swing angle and rely on the motion capture system dedicated for indoor condition[5][6].

\*This work was supported by the National Research Foundation of Korea (NRF) grant funded by the Korean government (MSIP) (2014R1A2A1A12067588).

Seung Jae Lee and H. Jin Kim are with the Department of Mechanical and Aerospace Engineering, Seoul National University, Gwanak-gu, Seoul, Korea [sjlazza@snu.ac.kr](mailto:sjlazza@snu.ac.kr), [hjinkim@snu.ac.kr](mailto:hjinkim@snu.ac.kr)



Fig. 1. Helicopter carrying bulky freight (left). The slung load concept also could be applied to multi-rotor UAVs (right) for various applications, but effects of the slung load should be carefully monitored in both cases.

Thus, when the motion capture system is not available (e.g. outdoor flight condition), it is impossible to stabilize the slung load based on its current swing angle state. Although alternatives without using the motion capture system can be conceived such as visual detection[9], they require extra sensor devices that cause a growth of the dry weight and the power consumption, or vulnerability to the environmental condition.

In this paper, we aim to develop a swing angle estimation method of the slung load without any external sensors except an attached IMU module and a single load cell. First, we construct an estimation algorithm of the disturbance force caused by the slung load in each axis using a unique application of the disturbance observer (DOB). Since the direction of the tension force is always same as the direction of the tether when it is taut, we can estimate the swing angle of the slung load from the estimated force components. In the end, we discuss the limitation of the method due to the uncertainty of the thrust mechanism and suggest a practical alternative using a single load cell. During the development of the algorithm, we will presume that the tether of the slung load is always taut.

This paper is organized as follows. In Section II, the system dynamics of UAV with slung-load attachment will be covered. In Section III, the computation of the swing angle will be described with the DOB-derived axial disturbance force estimation. In Section IV, both simulation and experimental results will be shown for validation of the suggested algorithm.

## II. SYSTEM DYNAMICS

In this section, we will brief about the dynamics of UAV. The first subsection presents the simplified UAV dynamics with several modifications in equation form, which will become the basis of our swing angle estimation algorithm in

section III. The second subsection describes the method to calculate the tension of the cable. Since it affects the dynamic behavior of two objects the UAV and the slung load, we should calculate the tension for simulation based on current states of two objects. The simulation was carried out based on true model with full dynamics of the UAV and slung load.

#### A. Dynamics of the UAV with and without Slung Load

Multi-rotor UAV dynamics is given by

$$\begin{cases} m\ddot{\mathbf{x}} = R(\mathbf{q})T_f + mg\mathbf{z}_e \\ J\dot{\boldsymbol{\Omega}} = T_m - \boldsymbol{\Omega} \times J\boldsymbol{\Omega} \end{cases} \quad (1)$$

where  $m$  is mass of the UAV,  $\mathbf{x} = [x \ y \ z]^T$  is position in the earth fixed frame,  $R(\mathbf{q})$  is the rotation matrix from the body frame to the earth fixed frame with  $\mathbf{q} = [\phi \ \theta \ \psi]^T$ , the roll, pitch, yaw attitude angles in the earth-fixed frame.  $T_f$  is the thrust torque vector in the body frame with  $T_f = [0 \ 0 \ -\Sigma F_i]^T$ , and  $g$  is gravitational acceleration.  $J$  is the moment of inertia,  $\boldsymbol{\Omega} = [p \ q \ r]^T$  is angular velocity in a body frame and  $T_m = [\tau_r \ \tau_p \ \tau_y]^T$  is the thrust torque vector in a body frame[8].

For stability, UAV's attitudinal motion is limited to  $\pm 0.3$  radian in both roll and pitch angle. This makes the gyroscopic effect of the airframe very small that it is permissible to neglect the term  $\boldsymbol{\Omega} \times J\boldsymbol{\Omega}$  in equation (1). It also makes the transform matrix  $W(\mathbf{q}) \approx I_{3 \times 3}$  in the following angular velocity coordinate transformation equation

$$\dot{\mathbf{q}} = W(\mathbf{q})\boldsymbol{\Omega} \approx \boldsymbol{\Omega} \quad (2)$$

[10]. Last, the  $\pm 0.3$  radian constraint makes the small angle assumption valid thus treatment of  $\sin(*) \approx *$  and  $\cos(*) \approx 1$  is permissible. In conclusion, equation (1) can be rewritten as

$$\begin{bmatrix} \ddot{x} \\ \ddot{y} \\ \ddot{z} \end{bmatrix} = \frac{1}{m} \begin{bmatrix} \Sigma F_i s\psi & \Sigma F_i c\psi & 0 \\ -\Sigma F_i c\psi & \Sigma F_i s\psi & 0 \\ 0 & 0 & \frac{-1}{m} c\phi c\theta \end{bmatrix} \begin{bmatrix} \phi \\ \theta \\ \Sigma F_i \end{bmatrix} + \begin{bmatrix} 0 \\ 0 \\ g \end{bmatrix} \quad (3)$$

for the translational dynamics and

$$\begin{bmatrix} \ddot{\phi} \\ \ddot{\theta} \\ \ddot{\psi} \end{bmatrix} = \begin{bmatrix} \frac{1}{J_{xx}} & 0 & 0 \\ 0 & \frac{1}{J_{yy}} & 0 \\ 0 & 0 & \frac{1}{J_{zz}} \end{bmatrix} \begin{bmatrix} \tau_r \\ \tau_p \\ \tau_r \end{bmatrix} \quad (4)$$

for the rotational dynamics. For conciseness, equations (3) and (4) are symbolized as

$$\begin{cases} \ddot{\mathbf{x}} = G(\mathbf{q}, \Sigma F_i)\boldsymbol{\Gamma} + g\mathbf{z}_e \\ \ddot{\mathbf{q}} = J^{-1}T_m \end{cases} \quad (5)$$

in further descriptions, where  $\boldsymbol{\Gamma} = [\phi \ \theta \ \Sigma F_i]^T$  is a state set for the UAV's control and  $G(\mathbf{q}, \Sigma F_i)$  is a relationship matrix between  $\ddot{\mathbf{x}}$  and  $\boldsymbol{\Gamma}$ .

Meanwhile, when the slung load is attached, tension of the tether acts as a disturbance force. With this aspect, adding an extra force and a torque term in equation (5) completes the equation. Rewriting equation (5), the dynamics of UAV could be written as

$$\begin{cases} \ddot{\mathbf{x}} = G(\mathbf{q}, \Sigma F_i)\boldsymbol{\Gamma} + g\mathbf{z}_e + \frac{1}{m}F_s \\ \ddot{\mathbf{q}} = J^{-1}(T_m + T_s) \end{cases} \quad (6)$$

where  $F_s = [F_{s,x} \ F_{s,y} \ F_{s,z}]^T$  and  $T_s = [T_{s,x} \ T_{s,y} \ T_{s,z}]^T$  are the disturbance force and torque, respectively, generated by the slung load. The concept of equation (6) gives a key idea of swing-angle estimation by deriving the relationship between  $F_s$  and the swing angle.

Meanwhile, the UAV dynamics for simulation should consider the full dynamics but also consider the slung load dynamics. Therefore, we should write the dynamics of the simulation as

$$\begin{cases} m\ddot{\mathbf{x}} = R(\mathbf{q})T_f + F_s + mg\mathbf{z}_e \\ J\dot{\boldsymbol{\Omega}} = T_m + T_s - \boldsymbol{\Omega} \times J\boldsymbol{\Omega} \end{cases} \quad (7)$$

However, equation (7) cannot be used to the simulation directly since the solution to calculate  $F_s$  and  $T_s$  over time is yet unknown.  $F_s$  and  $T_s$  are the force and torque generated by the mechanical constraint of the system. The mechanical constraint in our case is a constant length between UAV and a slung load. Therefore, we need to find out how to calculate  $F_s$  in each timestep, based on the length constraint for the simulation of both UAV and slung load.

#### B. Dynamics of the Slung-Load UAV for Simulation

The modelling of constraint dynamic system of the slung-load helicopter was studied for many years[11][12][13]. One of the most promising approaches is the Udwadia-Kalaba (U-K) equation[14]. The U-K equation is a dynamic equation based on the Gauss' principle of least constraint, where the system motion is governed by the acceleration vector of the system that is closest to the unconstrained acceleration while satisfying the constraint. In equation, it can be written as

$$\ddot{\zeta} = \arg \min \Delta(\ddot{\zeta}_\delta) \quad (8)$$

where  $\Delta(\ddot{\zeta}_\delta) = (\ddot{\zeta}_\delta - \ddot{\zeta}_u)^T M (\ddot{\zeta}_\delta - \ddot{\zeta}_u) = \Upsilon^T \Upsilon$  is the cost function to be minimized,  $\ddot{\zeta}_\delta$  represents all possible acceleration vectors,  $\ddot{\zeta}_u$  is the acceleration in free state without any physical constraints and  $M$  is the mass matrix.  $\Upsilon$  satisfying equation (8) and the constraint equation  $A\ddot{\zeta}_\delta = b$  is then

$$\Upsilon = (AM^{-\frac{1}{2}})^+(b - A\ddot{\zeta}_u) = M^{\frac{1}{2}}(\ddot{\zeta}_\delta - \ddot{\zeta}_u). \quad (9)$$

Therefore, the total force applied to the object is

$$F_{total} = M\ddot{\zeta} = F_u + F_c = M(\ddot{\zeta}_u + M^{-\frac{1}{2}}(AM^{-\frac{1}{2}})^+(b - A\ddot{\zeta}_u)) \quad (10)$$

where  $F_u = M\ddot{\zeta}_u$  is the unconstrained force and  $F_c = M^{\frac{1}{2}}(AM^{-\frac{1}{2}})^+(b - A\ddot{\zeta}_u)$  is the constraint force.

For the simulation of the slung-load UAV, the position vector is set to  $\zeta = [\mathbf{x}_h \ \mathbf{q}_h \ \mathbf{x}_l \ \mathbf{q}_l]^T$  where  $\mathbf{x}_h$  and  $\mathbf{q}_h$ ,  $\mathbf{x}_l$  and  $\mathbf{q}_l$  are the position and attitude of the UAV and the slung load respectively. The mass matrix  $M = \text{diag}(m_u I_{3 \times 3}, J_u, m_l I_{3 \times 3}, J_l)$  consists of  $m_u$  and  $J_u$ ,  $m_l$  and  $J_l$ , i.e. the mass and moment of the UAV and the slung load respectively. The unconstrained force is set to  $F_u = [[T_f + m_u g \mathbf{z}_e]^T \ T_m^T \ m_l g \mathbf{z}_e^T \ 0_{1 \times 3}]^T$ .

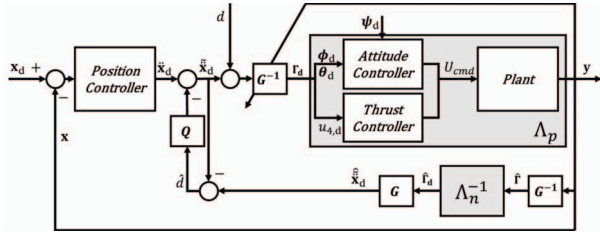


Fig. 2. Overall control scheme of UAV including position and attitude controller with acceleration-DOB algorithm.

### III. SWING-ANGLE ESTIMATION WITH AXIAL FORCE ESTIMATION

In this section, we will develop the swing angle estimation technique with slung load generated axial disturbance forces. Therefore, we need to estimate the disturbance force in each  $x_e$ ,  $y_e$  and  $z_e$  axis independently. In the first subsection, we will define the swing angle of the slung load. After then, we will develop a disturbance force estimation method by using the acceleration-DOB[10] in the second subsection. In the last subsection, we will cover the swing angle estimation utilizing the estimated disturbance force.

#### A. Definition of the Swing Angle

The swing angle is defined as follows. Two angles  $\alpha$  and  $\beta$  are defined as Fig. 3 shows.  $\alpha$  is the angle between  $z_e$  axis and the tether in  $(y_e - z_e)$  plane.  $\beta$  is the angle between  $z'_e$  axis and the tether in  $(x'_e - z'_e)$  plane, where the  $x'_e y'_e z'_e$  frame is the rotation of  $x_e y_e z_e$  in  $x_e$  axis so that the direction of  $z'_e$  is same as the slung load in  $(y_e - z_e)$  plane.

#### B. DOB-derived Disturbance Force Estimation

The DOB algorithm is originally developed for robust control of a system that is exposed to disturbance. The main idea of the DOB is to estimate the amount of disturbance and compensate it in the next step of control[7]. But instead of using the estimated disturbance for compensation, we are going to use it for monitoring how much disturbance force is generated by the slung load.

In [10], a DOB algorithm that aims to compensate lateral force disturbance has been introduced, which is a distinctive approach compared to the conventional application of DOB to UAVs that is targeted toward robustness of the attitude control. Therein, a lateral force control method was proposed by developing the lateral acceleration control of UAV in each axis. Acquiring the acceleration control of the UAV is essential for the implementation of DOB since the DOB algorithm requires an input command with same physical meaning to the disturbances that need to be compensated.

Fig. 2 shows the structure of the DOB-applied force control algorithm introduced in [10].  $\hat{\ddot{x}}_d$  in Fig. 2 is an overall acceleration command in each axis generated by adding disturbance compensation signal to the original acceleration command. This signal  $\hat{\ddot{x}}_d$  is then converted to  $\Gamma_d$  using

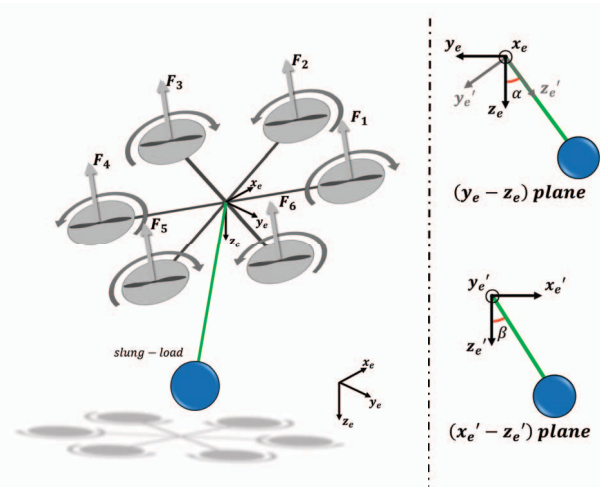


Fig. 3. Definition of the swing angle  $\alpha$  and  $\beta$ .  $\alpha$  is the angle between  $z_e$  and taut tether in  $(y_e - z_e)$  plane,  $\beta$  is the angle between the  $z'_e$  and taut tether in  $(y_e - z_e)$  plane.

equation (5) as

$$\Gamma_d = G^{-1}(\mathbf{q}, \Sigma F_i)(\hat{\ddot{x}}_d - g\mathbf{z}_e). \quad (11)$$

For the calculation of  $\Gamma_d$  with equation (11), the current total thrust  $\Sigma F_i$  is needed to figure out  $G^{-1}$ . But the acquisition of the precise thrust value is very difficult although many researches treated this value as a measurable output state. The uncertainty in  $\Sigma F_i$  is because of the imperfectness of the rotor dynamics and continuous battery voltage drop which makes electronic speed controller (ESC) difficult to maintain constant relationship between input command and output voltage/current. So, instead of mathematical model of the input-output thrust command relationship, an alternative method to estimate  $\Sigma F_i$  using equation (1) was introduced in [10]. The resultant  $T_f$  estimation is

$$T_f = mR^{-1}(\mathbf{q})(\hat{\ddot{x}} - g\mathbf{z}_e). \quad (12)$$

With this equation, the total thrust can be estimated since quantities needed for calculation are  $m$ ,  $\mathbf{q}$ ,  $\hat{\ddot{x}}$  and  $g$ , which are already known or measurable by an inertial measurement unit (IMU). By estimating total thrust, we can now calculate  $\Gamma_d$  in equation (11) which is an input command of  $\Lambda_p$  the gray box in Fig. 2 that consists of the hexacopter plant with attitude and thrust controllers ( $y = \Lambda_p \Gamma_d$ ).

In order to estimate the disturbance force,  $\hat{\ddot{x}}_d$  the estimation of  $\hat{\ddot{x}}_d + d$  should be calculated. The symbol  $\hat{\cdot}$  represents the estimated quantity throughout this paper. First,  $\hat{\Gamma}$  the estimation of  $\Gamma$  that causes current acceleration is calculated based on  $\hat{\ddot{x}}$ . At this time,  $\hat{\Gamma}$  could be significantly different from  $\Gamma$  since axial force disturbance hinders the nominal behavior of UAV. Then, the desired attitude command  $\hat{\Gamma}_d$  is calculated using  $\Lambda_n^{-1}$  the inverse of the nominal transfer function.  $\Lambda_n$  stands for the  $\Lambda_p$  in nominal situation. After that, the signal passes through  $G$  block in order to change  $\hat{\Gamma}_d$  to  $\hat{\ddot{x}}_d$  the estimated desired axial acceleration command, which also could be significantly different from

the real desired axial acceleration command because it is calculated based on  $\hat{\Gamma}_d$ . Finally,  $\hat{d}$  the estimated disturbance acceleration is calculated by

$$\hat{d} = \hat{\ddot{\mathbf{x}}}_d - \ddot{\mathbf{x}}_d = G(\mathbf{q}, \Sigma F_i) \Lambda_n^{-1} G^{-1}(\mathbf{q}, \Sigma F_i) \ddot{\mathbf{x}} - \ddot{\mathbf{x}}_d. \quad (13)$$

Since  $\hat{d}$  is the estimated amount of disturbed acceleration command that is compromised by the external influence, the disturbance force in each axis can be estimated by the multiplication of the mass to the estimated disturbance in each axis, which is

$$\hat{F}_s = m\hat{d}. \quad (14)$$

The force estimation is a key concept for development of the swing angle estimation in this paper. This method has a special meaning of treating  $\hat{d}$  not only as a lumped value used for enhancing the stability of the system, but as a value with physical meaning especially as an external force applied to the system by simple modification. Also, it is very practical since no other sensor but only IMU is needed for implementation.

We believe that this approach is a unique concept introduced in this paper to our best knowledge. But this method has a limitation in realization because of the imperfectness of the modern UAV hardware. In next subsection, we will discuss about the limitation and find out a remedy to overcome the problem.

### C. Overcoming the Physical Limit

One problem of the proposed disturbance force estimation is that accurate  $\mathbf{z}_e$  directional disturbance estimation is almost impossible. It is because the transfer function of the thrusters continuously changes compared to the  $\mathbf{x}_e$  and  $\mathbf{y}_e$  directional model, which is the same reason as the inaccuracy in estimating  $T_f$  introduced in the previous subsection. Thus, an alternative method to supplement this inaccuracy is needed.

The practical solution proposed in this paper is using a single load cell that measures tension force of the tether, which gives  $\|F_s\|$  the norm of the overall disturbance force generated by the slung load. Based on the swing-angle definition, the axial disturbance force in earth-fixed frame can be written as

$$\begin{cases} F_{s,x} = \|F_s\| \sin \beta \\ F_{s,y} = \|F_s\| \cos \beta \sin \alpha \\ F_{s,z} = \|F_s\| \cos \beta \cos \alpha \end{cases} \quad (15)$$

where  $F_{s,x}$ ,  $F_{s,y}$  and  $\|F_s\|$  are known values while  $F_{s,z}$  is not. However, despite the uncertainty of  $F_{s,z}$ , we are now able to calculate the swing angle because we can change the first two equations in equation (15) to

$$\begin{cases} \frac{F_{s,x}}{\|F_s\|} = \sin \beta \\ \frac{F_{s,y}}{\|F_s\|} = \cos \beta \sin \alpha \end{cases} \quad (16)$$

where all the variables in the left side of equations are known and two variables ( $\alpha$  and  $\beta$ ) can be obtained.

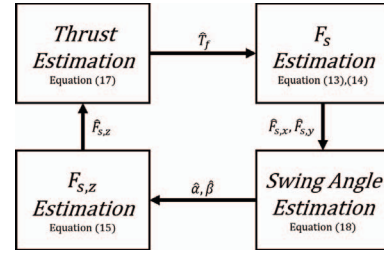


Fig. 4. Diagram of relationships among estimators. Each estimator needs estimation result of another estimator for calculation.

### D. Swing-Angle Estimation

Before we move to the swing-angle estimation, the DOB based  $F_{s,x}$ ,  $F_{s,y}$  estimation method introduced in section III-B should be modified to consider the slung load, because the dynamics has been changed from equation (5) to equation (6), thus the overall thrust estimation method introduced in equation (12) should be changed. The modified thrust estimation equation based on equation (7) is then

$$T_f = mR^{-1}(\mathbf{q})(\ddot{\mathbf{x}} - g\mathbf{z}_e - \frac{1}{m}F_s) \quad (17)$$

where  $F_s$  is added to the original equation. Therefore, we need a precise  $F_s$  estimation for good  $T_f$  estimation.

However, estimation of  $F_{s,x}$  and  $F_{s,y}$  in  $F_s$  needs precise estimation of  $T_f$  the total thrust since  $G(\mathbf{q}, \Sigma F_i)$  in equation (13) is using  $\Sigma F_i$  for the calculation. Meanwhile, the total thrust estimation also needs  $\hat{F}_{s,z}$  which is calculated with  $\hat{\alpha}$  and  $\hat{\beta}$ . Fig. 4 is a diagram showing the relationship among estimated values. Each of the four estimators has a dependency to another. However, the error of the thrust estimation in equation (17) is bounded since  $F_s$  does not exceed certain level during the flight. Therefore, the rest of estimators also have a limited output error. In later section, we can find out the performance of swing-angle estimation during the actual flight (Fig. 8).

Equation (16) can now be computed since we achieve good  $F_{s,x}$  and  $F_{s,y}$  estimation. And  $\|F_s\|$  is already known thanks to the load cell. Based on these, the swing-angle estimation is made as the following equation.

$$\begin{cases} \hat{\beta} = \arcsin\left(\frac{\hat{F}_{s,x}}{\|F_s\|}\right) \\ \hat{\alpha} = \arcsin\left(\frac{\hat{F}_{s,y}}{\|F_s\| \cos \hat{\beta}}\right) \end{cases} \quad (18)$$

It first estimates  $\beta$  because it is the only variable that can estimate with already known  $\hat{F}_{s,x}$ ,  $\hat{F}_{s,y}$  and  $\|F_s\|$ . Then,  $\hat{\alpha}$  is calculated with  $\hat{\beta}$ . The updated estimated swing angle is then used to calculate better  $\hat{F}_{s,z}$  with  $\hat{F}_{s,z} = \|F_s\| \cos \hat{\beta} \cos \hat{\alpha}$  in equation (15). It allows us to fill all the components in  $\hat{F}_s$  for more accurate  $T_f$  estimation.

## IV. SIMULATION AND EXPERIMENT

In this section, the simulation and experimental result of swing-angle estimation, which justifies the effectiveness and preciseness of the suggested algorithm, will be shown. In the first subsection, the simulation with consideration of the full

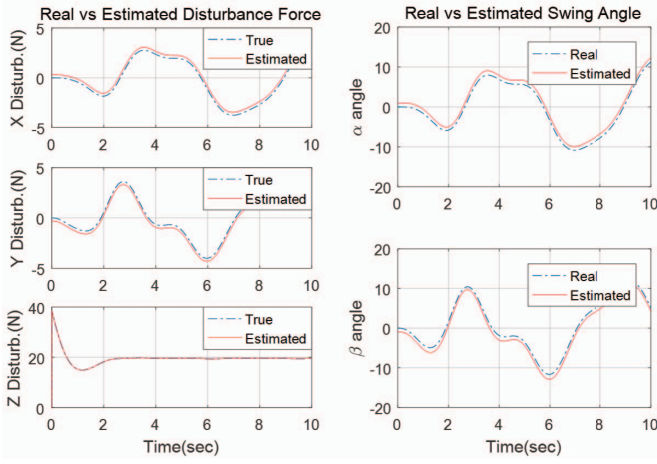


Fig. 5. Comparison between the estimated (red line) and true (blue line) disturbance force (left), swing angle (right) in the simulation environment

dynamics of the UAV and slung load using U-K equation for verification of the swing-angle estimation will be shown[9]. In the second subsection, experimental results of the swing-angle estimation will be presented with detailed experimental settings.

#### A. Simulation Result

The maneuver of the UAV during the simulation is set to follow the 2 m radius circular path, which slung load could constantly be exposed to the centripetal forces. Length of the tether is decided to be a 2 m with author's arbitrariness. U-K equation was adapted to figure out an interactive force and torque between the UAV and a slung load. Tension force ( $\|F_s\|$ ) based swing-angle estimation is performed for verification of the algorithm, even though the relationship between thrust command and actual thrust force is invariant of the time during the simulation. True swing-angle state for validation is calculated with

$$\begin{cases} \alpha = \arctan\left(\frac{\bar{x}}{\bar{z}}\right) \\ \beta = \arctan\left(\frac{\bar{y}}{\sqrt{\bar{x}^2 + \bar{y}^2}}\right) \end{cases} \quad (19)$$

where

$$\bar{\mathbf{x}} = \mathbf{x} - \mathbf{x}_{slungload} \quad (20)$$

that  $\bar{\mathbf{x}} = [\bar{x} \ \bar{y} \ \bar{z}]^T$  is the position error between UAV and a slung load. Fig. 5 shows a comparison between real and estimated disturbance forces and swing angles. As we can see, the proposed method shows the excellent performance of estimating the disturbance force during the flight. Therefore, the quality of the estimation of swing angle is acceptable compared to the real swing angle values. With the result, we could obtain the feasibility of the algorithm.

#### B. Experimental Result

The hexarotor UAV with 55 cm diameter fuselage and six 12 inch propellers is used for experiments. All the system codes are implemented in an on-board computer for fast response. The position and velocity data are obtained from

the VICON motion capture system, and sent to the on-board computer at 100Hz. The attitude data are retrieved from the built-in IMU at 500Hz. The flight control computer calculates the desired rotation speed for each motor. The current states are then sent to the ground controller for monitoring. The operator can set the desired position or gains of the controller using the uplink of the ground control system.

Our goal during the experiment is to monitor the swing angle over than 5 degrees. It is because the swing angle under 5 degrees is small enough not to cause concern over stability. For condition satisfactory, first we need to deal with disturbance force estimation noise because it is crucial for minimum resolution of the estimation angle. Fig. 6 is an experimental result of the disturbance force estimation without slung-load attachment, but pulled manually by human hand. The blue line represents the estimated force and the red line is for the sensor-measured force. When we magnify the time period from 75 to 79 seconds that is no-disturbance situation, the measurement has an error about  $\pm 1$  N regardless of any external disturbance force. This is because of the imperfectness of the estimation process in physical world in which the estimation algorithm cannot distinguish the actual force and noise within amount of  $\pm 1$ N in our case. The goal set for an experiment was to distinguish each swing angle with minimum 5 degrees as mentioned before. Therefore,  $F_{s,x}$  and  $F_{s,y}$  in equation (16) should be larger than 1N when each swing angle is 5 degrees. In equation, the relationship between  $\|F_s\|$  and  $\alpha_{min}, \beta_{min}$ , the minimum swing-angle resolution angle, could be written as

$$\begin{cases} \|F_s\| \geq \frac{\|F_{x,noise}\|}{\sin(\beta_{min})} \\ \|F_s\| \geq \frac{\|F_{y,noise}\|}{\sin(\alpha_{min}) \cos(\beta_{min})} \end{cases} \quad (21)$$

where  $\|F_{noise}\|$  is the standard level of noise of the estimated axial force generated regardless of the disturbance force in each axis, which is minimum 1 N in our case. Therefore,  $\|F_s\|$  the norm of the tension of the slung load should be larger than 11.5175 N and thus we need a slung load heavier

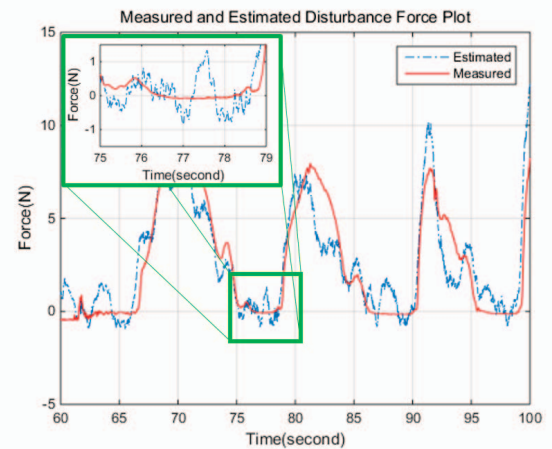


Fig. 6. Comparison between the estimated and true disturbance force in the experiment

than 1.1745 Kg of its own weight.

With consideration above, the slung load of 1.2 Kg is attached to the 1 m length tether. As we can see in Fig. 7, a load cell is installed in the middle of the tether for tensile force measurement. The marker for position information acquisition is attached to the slung load for true angle measurement. Fig. 8 shows a swing-angle estimation result with the altitude data during the flight. The UAV lifted off at 41 sec and reached the desired height 1.6 m at around 53 sec. The concave region around 43 sec in the  $Z$  position plot is due to the tether that just started to pull the fuselage right after the slung load is off the ground. Until around 55 sec, the swing-angle estimation was not so accurate because the stabilization of the internal estimation values denoted in Fig. 4 was not done yet. The system is set to have a 30 degree estimation angle limit in both  $\hat{\alpha}$  and  $\hat{\beta}$  angle estimators. The estimation performance is poor right after take off. But after 55 second when the height of UAV is regulated, the estimation becomes very accurate compared to the true  $\alpha$  and  $\beta$  values (blue lines). Thus, based on the result, we confirmed that the suggested algorithm is valid also in an experimental situation.

## V. CONCLUSIONS

In this paper, the swing-angle estimation method that does not need any external devices is introduced. For swing-angle calculation, a new external disturbance force estimation technique using only IMU sensor is developed. Also a practical solution, for implementation in real world involving uncertain elements such as thrust mechanism, is suggested by using the load cell attached in the middle of the tether. Both simulation and experiment are performed for validation, from which we are able to find out the validity and performance of the algorithm.

With the newly developed algorithm, the safety of UAVs flying with a slung load could become improved with efficiency using minimum additional sensor attachment. Furthermore, a similar approach can be useful for versatile applications by applying a disturbance force estimation technique to various UAV flights where interaction with environments is needed.

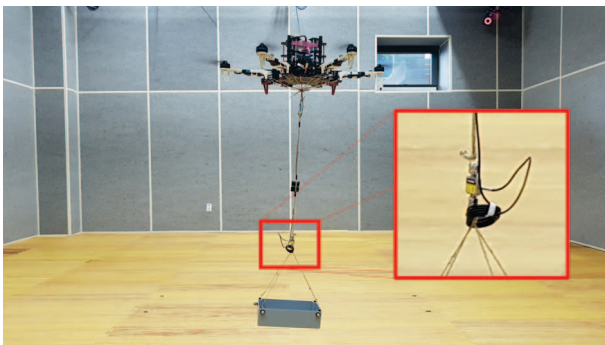


Fig. 7. Experimental setup of a UAV carrying a slung load. The inset shows that a load cell is attached in the middle of the tether for measurement of the overall disturbance force due to the slung load.

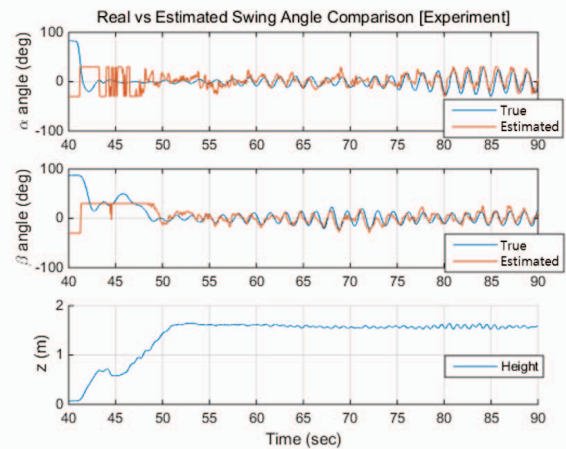


Fig. 8. Comparison between estimated (blue line) and real (red line) swing angle in the experimental environment.

## REFERENCES

- [1] Asseo, Sabi J., and Richard F. Whitbeck. "Control Requirements for Slung-Load Stabilization in Heavy Lift Helicopters." *Journal of the American Helicopter Society* 18.3 (1973): 23-31.
- [2] Pounds, Paul EI, Daniel R. Bersak, and Aaron M. Dollar. "Stability of small-scale UAV helicopters and quadrotors with added payload mass under PID control." *Autonomous Robots* 33.1-2 (2012): 129-142.
- [3] Palunko, Ivana, Patricio Cruz, and Rafael Fierro. "Agile load transportation: Safe and efficient load manipulation with aerial robots." *IEEE robotics and automation magazine* 19.3 (2012): 69-79.
- [4] Lee, Byung-Yoon, et al. "Study on payload stabilization method with the slung-load transportation system using a quad-rotor." *Control Conference (ECC), 2015 European. IEEE*, 2015.
- [5] Sreenath, Koushil, Nathan Michael, and Vijay Kumar. "Trajectory generation and control of a quadrotor with a cable-suspended load-A differentially-flat hybrid system." *Robotics and Automation (ICRA), 2013 IEEE International Conference on. IEEE*, 2013.
- [6] Palunko, Ivana, et al. "A reinforcement learning approach towards autonomous suspended load manipulation using aerial robots." *Robotics and Automation (ICRA), 2013 IEEE International Conference on. IEEE*, 2013.
- [7] Lee, Kooksun, Juhoon Back, and Ick Choy. "Nonlinear disturbance observer based robust attitude tracking controller for quadrotor UAVs." *International Journal of Control, Automation and Systems* 12.6 (2014): 1266-1275.
- [8] Hoffmann, Gabriel M., et al. "Quadrotor helicopter flight dynamics and control: Theory and experiment." *Proc. of the AIAA Guidance, Navigation, and Control Conference. Vol. 2. 2007.*
- [9] Bisgaard, Morten. *Modeling, estimation, and control of helicopter slung load system. Department of Control Engineering, Aalborg University, 2008.*
- [10] Lee, Seung Jae, et al. "Robust acceleration control of a hexarotor UAV with a disturbance observer." *Decision and Control (CDC), 2016 IEEE 55th Conference on. IEEE*, 2016.
- [11] Sampath, Prasad. *Dynamics of a Helicopter-Slung Load System, Maryland University, 1980. Diss. PhD Thesis.*
- [12] Ronen, Tuvya. "Dynamics of a helicopter with a sling load." *Dissertation Abstracts International Part B: Science and Engineering*, 47.5 (1986).
- [13] Cicolani, Luigi S., and Gerd Kanning. "Equations of motion of slung-load systems, including multilift systems." (1992).
- [14] Udawadia, Firdaus E., and Robert E. Kalaba. "A new perspective on constrained motion." *Proceedings: Mathematical and Physical Sciences* (1992): 407-410.